***Highlights (3 to 5 bullet points (maximum 85 characters including spaces per bullet point)**

- 41% of Cd in raw rice straw was exchangeable, posing great environmental risks
- Pyrolyzing at 300 °C did not significantly alter Cd fractions remained in biochar
- Exchangeable fraction of Cd dropped to 5.79% at 500 °C and to 2.12% at 700 °C
- Increasing temperature decreased exchangeable Cd fraction immobilized on biochar
- CRSB700 has the fastest and highest Cd removal, and most stable Cd immobilization

Risk evaluation of biochars produced from Cd-contaminated rice straw and optimization of its production for Cd removal

Zhengtao Shen[1,2,#], Xiaoliang Fan[3,#], Deyi Hou[1,*], Fei Jin[4], David O'Connor[1,*], Daniel C.W. Tsang[5], Yong Sik Ok[6], Daniel S. Alessi[2]

[1] School of Environment, Tsinghua University, Beijing 100084, China

[2] Department of Earth and Atmospheric Sciences, University of Alberta, Edmonton T6G 2E3, Canada

[3] School of Ecology and Environment, Inner Mongolia University, Hohhot 010021, China

[4] School of Engineering, University of Glasgow, Glasgow G12 8QQ, United Kingdom

[5] Department of Civil and Environmental Engineering, The Hong Kong Polytechnic University, Hung Hom, Kowloon, Hong Kong, China

[6] Korea Biochar Research Center & Division of Environmental Science and Ecological Engineering, Korea University, Seoul 02841, Republic of Korea

*Corresponding author:

Deyi Hou,

School of Environment, Tsinghua University, Beijing 100084, China

Tel. +86(10) 62781159; Fax: +86(10) 62781159

E-mail: houdeyi@tsinghua.edu.cn

&

David O'Connor

School of Environment, Tsinghua University, Beijing 100084, China

Tel. +86(10) 62781159; Fax: +86(10) 62781159

E-mail: d.m.oconnor@hotmail.com

[#] These authors contributed equally to this work

Abstract

Based on the “waste-treat-waste” concept, biochars were produced from cadmium (Cd)-contaminated rice straw (CRSBs) at 300, 500, and 700 °C (CRSB300, CRSB500, and CRSB700). The risks of the Cd remaining in CRSBs were evaluated and the optimal biochar pyrolysis temperature for Cd removal was investigated. It was observed that 41% of the total Cd in the raw rice straw was exchangeable, which may poses significant risks to crops and humans. Pyrolyzing at 300 °C did not significantly alter the Cd fractions, while the exchangeable fraction of Cd greatly dropped to 5.79% at 500 °C and further to 2.12% at 700 °C. Increasing the highest pyrolysis temperature resulted in CRSB with higher pH values, greater surface area, and smaller pore sizes, thus providing more rapid and efficient removal of Cd from aqueous solutions. For Cd removal tests, increasing pyrolysis temperature (300 to 700°C) increased the total (24.8 to 55.1 mg/g) and non-exchangeable (18.9 to 52.8 mg/g) Cd concentrations immobilized on the CRSBs and significantly decreased the exchangeable Cd fraction (23.7% to 4.85%). It is suggested based on the study from aqueous solutions that CRSB700 was the most suitable for the remediation of Cd contaminated soil on site due to the lowest risks of remained Cd from feedstock, fastest and highest Cd removal, and most stable immobilization of Cd.

Keywords

Sustainable waste management; cadmium rice; waste valorization/recycling; cadmium removal; green/sustainable remediation; pyrolysis temperature

1. Introduction

Land pollution is a global challenge in the modernization process (Hou et al., 2017a; O'Connor et al., 2018a; Hou and Ok, 2019). In 2014, China released its national soil survey results which indicated that 16.1% of the 6.3 million km^2 land surveyed and 19.4% of the surveyed cultivated land exceeded soil quality standards (Hou et al., 2017b). Heavy metals are of particular concern because it is non-degradable and tends to accumulate in surficial soil (Elbana et al., 2018; O'Connor et al., 2018b; Jin et al., 2019; Zhang et al., 2019). It is imperative to develop low-carbon, nature-based solutions (Wang et al., 2018; Song et al., 2019; Wang et al., 2019b), and green and sustainable remediation technologies to address heavy metal contamination (Zhang et al., 2018; Shen et al., 2019a; Wang et al., 2019c).

As the most widely distributed heavy metal contaminant, cadmium (Cd) is a chronic potent nephrotoxin and class one carcinogen (Clemens et al., 2013; Rizwan et al., 2016b). It is highly mobile in soils and can be easily accumulated in rice products. The rice grain, with elevated Cd, poses great health threats to humans through food chain. This “Cd rice” problem extensively exists globally, particularly in developing countries such as Bangladesh, India and China (Meharg et al., 2013; Rizwan et al., 2016a). Approximately 12 million tons of grains polluted by heavy metals were produced every year in China (Zhao and

92 Zhang, 2013). Among all the surveyed contaminants exceeding the soil quality
93 standards in China, the exceedance rate of Cd ranked number one, accounting
94 for 7.0% of total surveyed land (Liu et al., 2016). The elevated Cd content in soil
95 is the major culprit for the “Cd rice” problem. A survey conducted in Guangzhou
96 showed that 44% of the rice samples collected from an open market of the city
97 exceeded the health standards for Cd (Hou and Li, 2017).

98 In addition to rice grain that threatens people’s health, the “Cd rice” problem also
99 results in the generation of Cd contaminated rice straw. China produces ~200
100 million tonnes of rice grain annually, accounting for ~30% of world rice
101 production (Peng et al., 2009). The production of 1 tonne of rice grain can
102 generate approximately 1.5 tonnes of rice straw (Delivand et al., 2011).
103 Therefore, it can be estimated that ~300 million tonnes of rice straw is generated
104 annually and a large amount of these rice straws is contaminated by Cd.
105 Traditionally, rice straw, as an agricultural waste, can be utilized as fuel, feedstuff,
106 fertilizer, and industrial raw material (Liu et al., 2011). However, Cd
107 contamination in rice straw causes challenges in their disposal and utilization.
108 On one hand, it is a resource which can be potentially utilized in the field; on the
109 other hand, it is potentially hazardous and source of secondary contamination.

110 “Waste-treat-waste” technology is a popular trend in waste management and
111 environmental remediation (Chen et al., 2015; El Essawy et al., 2017; Wang et

al., 2019a). Following this concept, it would be of great environmental and economic benefits if the Cd contaminated rice straw could be used to remediate the Cd contaminated paddy soil on site. Pyrolyzing agricultural waste biomass to biochar is one of its most popular utilizations due to multiple benefits (Wang et al., 2017a; Wang et al., 2017b; El-Naggar et al., 2019). The original Cd in rice straws may pose risks to the environment, however, pyrolyzing may change the speciation of Cd in the rice straws and transform it into more stable forms with significantly lower environmental risks (von Gunten et al., 2017). Biochar typically has relatively high surface area, high alkalinity, active functional groups, and high aromaticity, and renders strong adsorption/immobilization ability for exogenous heavy metals under proper pyrolysis conditions and application circumstances (O'Connor et al., 2018c; Zhao et al., 2018; Chen et al., 2019). Pyrolysis temperature is a crucial factor affecting the environmental applications of biochar (Shen et al., 2019b; Sun et al., 2019). Although the effects of pyrolysis temperature on biochar properties have been extensively investigated (Kim et al., 2012; Zhang et al., 2017; Wei et al., 2019), few have looked at its influence on the chemical form, behavior and environmental risks of heavy metals in biochars. Huang et al. (2018) produced biochars from phytoremediation residue at three different temperatures (350, 550, and 750 °C), and observed that ~ 40% of the Cd and Zn in the biochars produced at 350 °C was mobile and had significant environmental risks. Pyrolyzing at 550 °C or higher can greatly reduce the

percentage of mobile Cd and Zn in the biochars and thereby reduce their risks. In addition, the influence of pyrolysis temperature on the adsorption mechanisms of heavy metals by biochars is very limitedly investigated. However, understanding this is of particular importance, because it is critical to find out the most suitable pyrolysis temperatures for the optimally environmental utilizations of biochar. Therefore, it is proposed to use biochars produced from Cd contaminated rice straw to treat Cd contaminated paddy soil on site. This solution offers advantages for: 1) reuse of waste, 2) abundant and readily available remediation material, 3) zero or little cost in material transportation, and 4) low life-cycle carbon footprint.

Before a large-scale application of this “waste-treat-waste” technology, two major issues remain unclear. Firstly, after pyrolyzing, the Cd stabilized in biochars may pose uncertain risks to the environment. It is important to evaluate whether pyrolyzing has successfully resulted in the immobilization of the Cd in the raw rice straws. Secondly, it is crucial to find the optimal pyrolysis condition for the most effective utilization of Cd contaminated rice straw biochar for Cd farmland soil remediation. In view of these considerations, biochars were produced from Cd contaminated rice straw at different temperatures. The mobility and risks of remained Cd in the biochars were investigated. In addition, the ability of the produced biochar to remove/immobilize Cd from aqueous solutions was investigated. This study aims to provide fundamental insights into

the feasibility of using Cd contaminated rice straw to treat Cd contaminated paddy soil on site.

2. Materials and methods

2.1. Biochar

The Cd contaminated rice straws (CRSs) (pH 6.74) were harvested from a farmland in Taicang, Suzhou, China. The paddy soil where the rice straw grew was contaminated by Cd (1.99 mg kg^{-1}) due to a range of reasons: industrial Cd discharge, waste disposal, and the usage of Cd-containing nitrogen fertilizer. After reception, the rice straws were dried in an oven at 60 °C to reach a constant weight.

Biochars were produced from the rice straws at three different temperatures (300, 500, and 700 °C) based on previous studies (Yuan et al., 2014; Zhao et al., 2018; Wei et al., 2019) in a furnace (QSX-4-12, CINITE, China) with limited air. The heating rate and residence time were fixed at 10 °C/min and 1 h, respectively, resulting in three biochars named CRSB300, CRSB500, and CRSB700, respectively. After production, the physicochemical properties, molecular structure, and mineral composition of the biochars were determined. The details of the characterization methods are shown in supporting information (SI).

2.2. Risk evaluation

In order to evaluate the risks of the biochars produced from Cd contaminated rice straw, the exchangeable and non-exchangeable fractions (fractions with binding energy stronger than ion exchange) of the original Cd remained in the biochars were determined and compared with that in the raw rice straw. Briefly, a certain amount of biochar (0.1 g) was added to 0.5 M $MgCl_2$ (8 mL) (pH 7.0). The mixture was shaken for 20 min (250 rpm) under room temperature (Shen et al., 2017a). After centrifugation, the supernatants was filtered using 0.45 μm filter, and the Cd concentrations was determined by inductively coupled plasma optical emission spectrometry (ICP-OES) test after acidification. The non-exchangeable fraction of Cd in the biochars was obtained by subtracting the exchangeable fraction from the total Cd. The total Cd concentration of biochar was tested according to USEPA 3051 method. Briefly, a certain amount of biochar (0.25 g) was added to 9 mL of 68% (w/w) nitric acid and 3 mL of 36% (w/w) hydrochloric acid. The mixture was digested for 25 min (5 min (120 °C) + 10 min (150 °C) + 10 min (180 °C)) in a MARS6 Microwave digestion system (CEM, United States). After cooling to room temperature, the residual solution was filtered using 0.45 μm filter and diluted for ICP-OES test of Cd.

2.3 Cd removal studies and speciation determination of immobilized Cd

In order to assess the performance of the produced biochars in Cd

193 removal/immobilization, the kinetics and equilibrium studies were conducted.
194 Pseudo first order, pseudo second order, and intraparticle diffusion model were
195 applied for kinetics data fitting. Langmuir and Freundlich models were used to fit
196 the equilibrium data. The details of these tests and data fitting can be found in
197 SI.

198 After Cd removal, the biochar samples in initial 5 mM (equivalent to 562 mg L^{-1})
199 Cd solutions were separated from solution through centrifugation and filtration.
200 The biochars were dried in an oven at 60 °C to reach a constant weight. The
201 exchangeable and non-exchangeable Cd immobilized on the biochars were
202 determined as per section 2.2. The dried samples were also analyzed by
203 Fourier-transform infrared spectroscopy (FTIR) and X-ray diffraction (XRD) to
204 reveal the molecular and mineralogical changes respectively.

205 2.4. Statistical analysis

206 The chemical experiments were carried out in duplicate, and the mean and
207 standard deviations were presented. FTIR and XRD tests were carried out once
208 and therefore statistical analysis was not conducted for these tests.

209 3. Results and discussion

210 3.1 Biochar properties

211 The properties of the biochars are presented in Table 1. CRSB500 and

212 CRSB700 were alkaline with pH values of 10.4 and 11.5, while CRSB300 was
213 nearly neutral with a pH of 7.50. The carbon content (49.9-53.3%) increased with
214 increasing pyrolysis temperature. In contrast, the contents of H, N, and O and
215 biochar yields dropped as the pyrolysis temperature increased. These resulted
216 from the higher degree of dehydration at higher pyrolysis temperatures, which
217 also lead to less hydrophilicity and higher aromaticity for the biochars (reflected
218 by decreased H/C and O/C values) (Zhao et al., 2017).

219 The BET surface areas for the biochars significantly increased with increasing
220 pyrolysis temperature. In particular, as pyrolysis temperature rose from 500 to
221 700°C, the BET surface area dramatically rose from 3.80 to 188 m^2/g;
222 meanwhile, the average pore width dropped from 40.3 to 6.98 nm. The pore size
223 distribution of the biochars is shown in Figure S1. The pore width of CRSB300,
224 CRSB500, and CRSB700 is approximately within 30-200, 7-200, and 2-200 nm.
225 The surface morphology also shows that the pore diameters of CRSB700 were
226 significantly smaller than CRSB300 and CRSB500 (Figure 1). Increasing
227 pyrolysis temperature enhanced the volatilization of organic matter in biochar
228 and therefore created more pores, resulting in increased surface area (Zhao et
229 al., 2018). The pore width significantly decreased, because macro-pores were
230 destroyed and meso- and micro- pores formed at higher pyrolysis temperatures
231 due to increased degree of volatilization (Keiluweit et al., 2010). The formation of
232 meso- and micro- pores greatly aid the increase of surface area at higher

pyrolysis temperature (700°C).

The FTIR spectra of the biochars are shown in Figure 2. For CRSB300, the peak at 1700 cm^{-1} represents C=O stretching, which originates from carboxyl group. The peak at 1610 cm^{-1} is assigned to aromatic C=C stretching. The peaks at 785 and 670 cm^{-1} are attributed to aromatic C-H out-of-plane deformation, which is also typically observed for biochars. The FTIR spectra of CRSB500 are similar to CRSB300. But two new peaks emerge at 1410 cm^{-1} and 875 cm^{-1}, representing aromatic C=C stretching and aromatic C-H out-of-plane deformation, respectively. This was due to the higher degree of aromatization as the pyrolysis temperature increased to 500 °C. For CRSB700, all the peaks weakened due to a larger degree of condensation for the aromatic units at 700 °C (Keiluweit et al., 2010). The peak at 1320 cm^{-1} represents the O-H bending of phenols. The peaks at 1030-1090 cm^{-1} are the combination of aliphatic C-O peak and Si-O-Si peak (Keiluweit et al., 2010; Shen et al., 2017b). With increased pyrolysis temperature, the C-O peak gradually diminished due to the decomposition of aliphatic organics and Si-O-Si peak strengthened due to the formation of SiO_2, resulting in the shift of the peaks at 1030-1090 cm^{-1} to the right.

The XRD patterns of the biochars are shown in Figure 3. Peaks representing sylvine (KCl) were observed for all biochars, which coincides with previous studies that biochar produced from rice straw contained KCl (Shen et al., 2019b).

253 A peak associated with calcite ($CaCO_3$) was observed for CRSB500 and
254 CRSB700. This peak diminished at 700 °C because $CaCO_3$ decomposed at
255 higher pyrolysis temperatures. This peak was not observed for CRSB300,
256 because the carboxylates in biochar did not start carbonization at such lower
257 temperatures (Dodson, 2011). Nitratine ($NaNO_3$) was observed on the biochars
258 after Cd removal, because excessive $NaNO_3$ (0.01 M) was added to Cd solution
259 to control constant ionic strength for the Cd removal tests and some of them
260 remained on biochar surface. In general, the XRD patterns show amorphous
261 carbon structure of the biochars.

262 3.2 Risks of Cd remained in the biochars

263 After pyrolysis, Cd in the raw rice straw remained in the produced biochars. The
264 concentrations were within 0.89-1.04 mg kg^{-1}, whereas that of raw rice straw
265 was 0.42 mg kg^{-1} (Figure 4). The concentrations of Cd in the biochar were higher
266 than that of raw rice straw, because the organics in the biomass volatilized and
267 the total mass decreased; meanwhile, the mass of Cd remained unchanged.
268 The exchangeable and non-exchangeable fractions of the remained Cd are
269 shown in Figure 4a. It can be observed that 41% of the total Cd in the raw rice
270 straw was exchangeable. This fraction of Cd is readily bioavailable in soil
271 environment and poses great risks to plants and humans (Filgueiras et al., 2002;
272 Shen et al., 2017a). Pyrolyzing at 300 °C did not significantly alter the

273 percentage of exchangeable Cd (37.2%), suggesting that the risks still exist for
274 CRSB300. As pyrolysis temperature increased, the percentage of exchangeable
275 Cd among total Cd in the biochars greatly dropped to 5.79% at 500 °C and
276 further to 2.12% at 700 °C.

277 Therefore, it can be concluded that the risks of Cd remained in the biochars can
278 be significantly reduced when pyrolysis temperature increased to 500 °C or
279 higher. Because the alkalinity of the biochar was enhanced at higher
280 temperatures which aided the immobilization of Cd in the biochar through
281 buffering effect (Inyang et al., 2015), and the exchangeable Cd was shifted to
282 precipitated and other more stable forms. The Cd may also exist in more stable
283 mineral forms at higher pyrolysis temperatures (Dodson, 2011). In comparison,
284 the produced biochar at 300 °C has active functional groups (e.g., hydroxyl and
285 carboxylic groups) (Dodson, 2011), and Cd may exchange with H^+ from these
286 groups which resulted in the higher percentage of exchangeable Cd in
287 CRSB300. It is of note that although the percentage fraction of exchangeable Cd
288 of CRS and CRSB300 is similar, the concentration of exchangeable Cd of
289 CRSB300 is higher than CRS (Figure 4b). This was partly due to the loss of
290 volatile organics for CRSB300 which concentrated the Cd in biochar. At 500 °C
291 and 700 °C, the majority of exchangeable Cd in CRS was converted to
292 non-exchangeable fraction, therefore the overall Cd concentration in CRSB500
293 and CRSB700 was significantly lower than CRS regardless the loss of the

294 volatile matter. The findings are in line with Huang et al. (2018) that increasing
295 pyrolysis temperature from 350 to 750 °C decreased the mobile (exchangeable)
296 fraction of Cd and increased the stable fractions of Cd for a phytoremediation
297 residue biochar. Bian et al. (2018) pyrolyzed Cd contaminated wheat straws at
298 350 and 550 °C and observed that the acid soluble Cd in the biochars was very
299 low to negligible. However, both the present study and Huang et al. (2018) found
300 that the biochars produced at low temperatures (300 and 350 °C) contained
301 significantly amount of exchangeable Cd and posed environmental risks.

302 3.3 Speciation of Cd immobilized on the biochars

303 After Cd removal from the aqueous solution in the batch tests, the fractions of
304 immobilized Cd on the biochars are shown in Figure 5a. The exchangeable Cd
305 fraction was 23.7% and 15.1% among total immobilized Cd on CRSB300 and
306 CRSB500, respectively. It significantly dropped to 4.85% when pyrolysis
307 increased to 700 °C. The immobilized Cd concentration on the biochars is shown
308 in Figure 5b. Similarly, the exchangeable Cd concentration was 5.86 and 6.13
309 mg/g on CRSB300 and CRSB500, respectively. In comparison, this
310 concentration for CRSB700 was significantly lower (2.67 mg/g). It can also be
311 observed that both total immobilized Cd (24.8-55.1 mg/g) and
312 non-exchangeable Cd (18.9-52.8 mg/g) concentrations for the biochars
313 significantly increased with increasing pyrolysis temperature from 300 to 700 °C.

314 It can be observed from the XRD patterns (see Figure 3) that $CdCO_3$ formed on
315 CRSB500 and CRSB700 after batch adsorption tests. The peaks representing
316 $CdCO_3$ are much stronger in CRSB700, suggesting its higher concentrations of
317 $CdCO_3$ compared with CRSB300 and CRSB500. This finding coincides with
318 previous observations that higher alkalinity of biochar favors the formation of Cd
319 precipitates such as $CdCO_3$ (Zhang et al., 2015). Therefore, the increased
320 precipitation of Cd contributed to the increase of both total immobilized Cd and
321 non-exchangeable Cd concentrations for biochars at higher pyrolysis
322 temperatures. No significant differences were observed from the FTIR spectra of
323 the biochars before and after Cd immobilization (Figure 2).

324 3.4 Kinetics and capacity of Cd removal by the biochars

325 The removal kinetics of Cd by the biochars are presented in Figure 6a and Table
326 2. Pseudo second order model generally better describes the kinetics results,
327 and the equilibrium adsorption capacities (q_e) obtained by this model fitting are in
328 the order of CRSB300<CRSB500<CRSB700 (23.8, 38.2, and 50.8 mg/g,
329 respectively). In addition to the lowest q_e value, CRSB300 also has the slowest
330 removal kinetics. At 5 min, Cd amount equivalent to 6.6% of q_e was removed,
331 and the removal achieved 79.2% of q_e at 6 h. In comparison, Cd amount
332 equivalent to 62.3 and 64.6% of q_e was removed by CRSB500 and CRSB700
333 respectively at 5 min, and the values climbed to 76.3% and 87.6% respectively

334 at 30 min. These results suggest that higher pyrolysis temperature in the range
335 of 300-700 °C significantly promoted both the amount and kinetics of Cd removal
336 by the CRS biochars.

337 Intraparticle diffusion model is typically used to fit the kinetics data to reveal the
338 film and intraparticle diffusion features. The intraparticle diffusion modelling
339 results are shown in Figure 6b and Table 2. It can be observed that both film and
340 intraparticle diffusion exist in the adsorption of Cd to the biochars, and
341 intraparticle is the primary rate-limiting step.

342 The equilibrium results are shown in Figure 7 and Table 3. Langmuir model
343 generally described the equilibrium data better compared with Freundlich model
344 for all biochars. The calculated maximum adsorption capacity (Q_{max}) values are
345 in the order of CRSB300<CRSB500<CRSB700 (21.4, 44.2, and 65.5 mg/g,
346 respectively). This further suggests that higher pyrolysis temperature in the
347 range of 300-700 °C facilitated the removal capacity of CRS biochars for Cd.
348 This coincides with the findings from previous studies that increasing pyrolysis
349 temperature generally increase the removal of heavy metals by biochars (Shen
350 et al., 2017b; Shen et al., 2019b).

351 3.5 Environmental implications

352 In field conditions, the exchangeable Cd are readily available to plants and may
353 be easily absorbed by crops (e.g., rice and wheat) threatening human's health

354 through ingestion (Filgueiras et al., 2002). They may also migrate through
355 rainfall and groundwater flow under slightly acidic environment, and thereby
356 pose further risks (Shen et al., 2018a; Shen et al., 2018b). This study observed
357 that the immobilized Cd on CRSB700 has the lowest exchangeable fraction. In
358 addition, the remaining Cd from the raw rice straw also revealed the lowest
359 exchangeable Cd fraction in CRSB700. Considering the highest Cd removal
360 capacity, it can be concluded that the biochar produced from Cd contaminated
361 rice straw at 700 °C is most suitable and has huge potential to be applied in
362 green remediation and in-situ stabilization of Cd contaminated soil. However, the
363 real performance of the biochars in Cd immobilization in field soils also depends
364 on the soil texture, soil organic matter, and other environmental factors
365 (El-Naggar et al., 2018; Shen et al., 2018a).

366 It is of note that although CRSB300 and CRSB500 may not be suitable for soil
367 remediation due to the relatively high exchangeable Cd fraction immobilized on
368 them, they may be suitable for water treatment of Cd. It is very important for the
369 recharge and reuse of adsorbents during water treatment in order for a high
370 cost-efficiency. The weakly bonded Cd on the biochar is easily to be discharged
371 (e.g., by slightly adjusting the environmental pH), and therefore the biochar may
372 be reused for many times.

4. Conclusions

It was observed that 41% of the total Cd in the raw rice straw was exchangeable which may poses great risks to crops and humans. Pyrolyzing at 300 °C did not significantly alter the Cd fractions, but the exchangeable fraction of Cd greatly dropped to 5.79% at 500 °C and further to 2.12% at 700 °C. Higher pyrolysis temperature results in CRSBs with higher pH values, higher surface areas, smaller pore sizes, and faster and higher Cd removal from aqueous solutions. For Cd removal studies, the calculated maximum adsorption capacity (Q_{max}) values are in the order of CRSB300<CRSB500<CRSB700. Increasing pyrolysis temperature (300 to 700°C) increased the total and non-exchangeable and Cd concentrations immobilized on the CRSBs and significantly decreased the exchangeable Cd fraction. It can be concluded that CRSB700 was the most suitable for the remediation of Cd contaminated soil on site due to 1) the lowest risks of remained Cd from feedstock, 2) fastest and highest Cd removal, and 3) the most stable immobilization of Cd.

Acknowledgements

This work was supported by China's National Water Pollution Control and Treatment Science and Technology Major Project (Grant No. 2018ZX07109-003), and the National Key Research and Development Program of China (Grant No. 2018YFC1801300). The first author would like to thank the Killam Trusts of

Canada for kindly providing the Izaak Walton Killam Memorial Postdoctoral Fellowship.

References

Bian, R., Li, L., Shi, W., Ma, B., Joseph, S., Li, L., Liu, X., Zheng, J., Zhang, X., Cheng, K., Pan, G., 2018. Pyrolysis of contaminated wheat straw to stabilize toxic metals in biochar but recycle the extract for agricultural use. Biomass & Bioenergy 118, 32-39.

Chen, C., Yu, J., Yoza, B.A., Li, Q.X., Wang, G.J.J.o.e.m., 2015. A novel "wastes-treat-wastes" technology: Role and potential of spent fluid catalytic cracking catalyst assisted ozonation of petrochemical wastewater. 152, 58-65.

Chen, L., Wang, L., Cho, D.-W., Tsang, D.C., Tong, L., Zhou, Y., Yang, J., Hu, Q., Poon, C.S., 2019. Sustainable stabilization/solidification of municipal solid waste incinerator fly ash by incorporation of green materials. Journal of Cleaner Production.

Clemens, S., Aarts, M.G., Thomine, S., Verbruggen, N.J.T.i.p.s., 2013. Plant science: the key to preventing slow cadmium poisoning. 18, 92-99.

Delivand, M.K., Barz, M., Gheewala, S.H., 2011. Logistics cost analysis of rice straw for biomass power generation in Thailand. Energy 36, 1435-1441.

Dodson, J., 2011. Wheat straw ash and its use as a silica source. University of York.

El-Naggar, A., Lee, S.S., Rinklebe, J., Farooq, M., Song, H., Sarmah, A.K., Zimmerman, A.R., Ahmad, M., Shaheen, S.M., Ok, Y.S., 2019. Biochar application to low fertility soils: A review of current status, and future prospects. Geoderma 337, 536-554.

El-Naggar, A., Shaheen, S.M., Ok, Y.S., Rinklebe, J., 2018. Biochar affects the dissolved and colloidal concentrations of Cd, Cu, Ni, and Zn and their phytoavailability and potential mobility in a mining soil under dynamic redox-conditions. Science of the Total Environment 624, 1059-1071.

El Essawy, N.A., Ali, S.M., Farag, H.A., Konsowa, A.H., Elnouby, M., Hamad, H.A., 2017. Green synthesis of graphene from recycled PET bottle wastes for use in the adsorption of dyes in aqueous solution. Ecotox Environ Safe 145, 57-68.

Elbana, T.A., Selim, H.M., Akrami, N., Newman, A., Shaheen, S.M., Rinklebe, J., 2018. Freundlich sorption parameters for cadmium, copper, nickel, lead, and zinc for different soils: Influence of kinetics. Geoderma 324, 80-88.

Filgueiras, A.V., Lavilla, I., Bendicho, C., 2002. Chemical sequential extraction for metal partitioning in environmental solid samples. Journal of Environmental Monitoring 4, 823-857.

Hou, D., Li, F., 2017. Complexities Surrounding China's Soil Action Plan. Land Degradation & Development 28, 2315-2320.

Hou, D., O'Connor, D., Nathanail, P., Tian, L., Ma, Y., 2017a. Integrated GIS and multivariate statistical analysis for regional scale assessment of heavy metal soil contamination: A critical review. Environmental Pollution 231, 1188-1200.

Hou, D., Ok, Y.S., 2019. Soil pollution — speed up global mapping. Nature 566, 455.

Hou, D.Y., O'Connor, D., Nathanail, P., Tian, L., Ma, Y., 2017b. Integrated GIS and multivariate statistical analysis for regional scale assessment of heavy metal soil

contamination: A critical review. Environmental Pollution 231, 1188-1200.

Huang, H., Yao, W., Li, R., Ali, A., Du, J., Guo, D., Xiao, R., Guo, Z., Zhang, Z., Awasthi, M.K.J.B.t., 2018. Effect of pyrolysis temperature on chemical form, behavior and environmental risk of Zn, Pb and Cd in biochar produced from phytoremediation residue. 249, 487-493.

Inyang, M.I., Gao, B., Yao, Y., Xue, Y., Zimmerman, A., Mosa, A., Pullammanappallil, P., Ok, Y.S., Cao, X., 2015. A review of biochar as a low-cost adsorbent for aqueous heavy metal removal. Critical Reviews in Environmental Science and Technology 46, 406-433.

Jin, Y., O'Connor, D., Ok, Y.S., Tsang, D.C., Liu, A., Hou, D., 2019. Assessment of sources of heavy metals in soil and dust at children's playgrounds in Beijing using GIS and multivariate statistical analysis. Environment international 124, 320-328.

Keiluweit, M., Nico, P.S., Johnson, M.G., Kleber, M., 2010. Dynamic Molecular Structure of Plant Biomass-Derived Black Carbon (Biochar). Environmental Science & Technology 44, 1247-1253.

Kim, K.H., Kim, J.Y., Cho, T.S., Choi, J.W., 2012. Influence of pyrolysis temperature on physicochemical properties of biochar obtained from the fast pyrolysis of pitch pine (Pinus rigida). Bioresour Technol 118, 158-162.

Liu, X., Tian, G., Jiang, D., Zhang, C., Kong, L.J.E.S., Research, P., 2016. Cadmium (Cd) distribution and contamination in Chinese paddy soils on national scale. 23, 17941-17952.

Liu, Z., Xu, A., Long, B.J.E., Engineering, P., 2011. Energy from combustion of rice

straw: status and challenges to China. 3, 325.

Meharg, A.A., Norton, G., Deacon, C., Williams, P., Adomako, E.E., Price, A., Zhu, Y.G., Li, G., Zhao, F.J., McGrath, S., Villada, A., Sommella, A., De Silva, P.M.C.S., Brammer, H., Dasgupta, T., Islam, M.R., 2013. Variation in Rice Cadmium Related to Human Exposure. Environmental Science & Technology 47, 5613-5618.

O'Connor, D., Hou, D., Ok, Y.S., Song, Y., Sarmah, A., Li, X., Tack, F.M., 2018a. Sustainable in situ remediation of recalcitrant organic pollutants in groundwater with controlled release materials: A review. Journal of Controlled Release 283, 200-213.

O'Connor, D., Hou, D., Ye, J., Zhang, Y., Ok, Y.S., Song, Y., Coulon, F., Peng, T., Tian, L., 2018b. Lead-based paint remains a major public health concern: A critical review of global production, trade, use, exposure, health risk, and implications. Environment international 121, 85-101.

O'Connor, D., Peng, T., Zhang, J., Tsang, D.C., Alessi, D.S., Shen, Z., Bolan, N.S., Hou, D., 2018c. Biochar application for the remediation of heavy metal polluted land: A review of in situ field trials. Science of The Total Environment 619, 815-826.

Peng, S.B., Tang, Q.Y., Zou, Y.B., 2009. Current Status and Challenges of Rice Production in China. Plant Production Science 12, 3-8.

Rizwan, M., Ali, S., Abbas, T., Zia-ur-Rehman, M., Hannan, F., Keller, C., Al-Wabel, M.I., Ok, Y.S., 2016a. Cadmium minimization in wheat: a critical review. Ecotox Environ Safe 130, 43-53.

Rizwan, M., Ali, S., Adrees, M., Rizvi, H., Zia-ur-Rehman, M., Hannan, F., Qayyum,

476 M.F., Hafeez, F., Ok, Y.S., 2016b. Cadmium stress in rice: toxic effects, tolerance
477 mechanisms, and management: a critical review. Environmental Science and Pollution
478 Research 23, 17859-17879.
479 Shen, Z., Hou, D., Xu, W., Zhang, J., Jin, F., Zhao, B., Pan, S., Peng, T., Alessi,
480 D.S.J.S.o.t.t.e., 2018a. Assessing long-term stability of cadmium and lead in a soil
481 washing residue amended with MgO-based binders using quantitative accelerated
482 ageing. Science of The Total Environment 643, 1571-1578.
483 Shen, Z., Hou, D., Zhao, B., Xu, W., Ok, Y.S., Bolan, N.S., Alessi, D.S., 2018b. Stability
484 of heavy metals in soil washing residue with and without biochar addition under
485 accelerated ageing. Sci Total Environ 619-620, 185-193.
486 Shen, Z., Zhang, J., Hou, D., Tsang, D.C.W., Ok, Y.S., Alessi, D.S., 2019a. Synthesis of
487 MgO-coated corncob biochar and its application in lead stabilization in a soil washing
488 residue. Environment international.
489 Shen, Z., Zhang, Y., Jin, F., McMillan, O., Al-Tabbaa, A., 2017a. Qualitative and
490 quantitative characterisation of adsorption mechanisms of lead on four biochars. Sci
491 Total Environ 609, 1401-1410.
492 Shen, Z., Zhang, Y., McMillan, O., Jin, F., Al-Tabbaa, A., 2017b. Characteristics and
493 mechanisms of nickel adsorption on biochars produced from wheat straw pellets and
494 rice husk. Environ Sci Pollut Res Int 24, 12809-12819.
495 Shen, Z.T., Hou, D.Y., Jin, F., Shi, J.X., Fan, X.L., Tsang, D.C.W., Alessi, D.S., 2019b.
496 Effect of production temperature on lead removal mechanisms by rice straw biochars.

497 Science of the Total Environment 655, 751-758.
498 Song, Y., Kirkwood, N., Maksimović, Č., Zhen, X., O'Connor, D., Jin, Y., Hou, D., 2019.
499 Nature based solutions for contaminated land remediation and brownfield
500 redevelopment in cities: A review. Science of The Total Environment.
501 Sun, Y., Iris, K., Tsang, D.C., Cao, X., Lin, D., Wang, L., Graham, N.J., Alessi, D.S.,
502 Komárek, M., Ok, Y.S., 2019. Multifunctional iron-biochar composites for the removal of
503 potentially toxic elements, inherent cations, and hetero-chloride from hydraulic
504 fracturing wastewater. Environment international 124, 521-532.
505 von Gunten, K., Alam, M.S., Hubmann, M., Ok, Y.S., Konhauser, K.O., Alessi, D.S.,
506 2017. Modified sequential extraction for biochar and petroleum coke: Metal release
507 potential and its environmental implications. Bioresource Technol 236, 106-110.
508 Wang, H., Chu, Y.X., Fang, C.R., Huang, F., Song, Y.L., Xue, X.D., 2017a. Sorption of
509 tetracycline on biochar derived from rice straw under different temperatures. Plos One
510 12.
511 Wang, L., Chen, L., Cho, D.-W., Tsang, D.C., Yang, J., Hou, D., Baek, K., Kua, H.W.,
512 Poon, C.-S., 2019a. Novel synergy of Si-rich minerals and reactive MgO for
513 stabilisation/solidification of contaminated sediment. Journal of hazardous materials 365,
514 695-706.
515 Wang, L., Cho, D.-W., Tsang, D.C., Cao, X., Hou, D., Shen, Z., Alessi, D.S., Ok, Y.S.,
516 Poon, C.S., 2019b. Green remediation of As and Pb contaminated soil using
517 cement-free clay-based stabilization/solidification. Environment international 126,

518 336-345.

519 Wang, L., Yu, K., Li, J.-S., Tsang, D.C., Poon, C.S., Yoo, J.-C., Baek, K., Ding, S., Hou,

520 D., Dai, J.-G., 2018. Low-carbon and low-alkalinity stabilization/solidification of high-Pb

521 contaminated soil. Chemical Engineering Journal 351, 418-427.

522 Wang, X., Liu, N., Liu, Y., Jiang, L., Zeng, G., Tan, X., Liu, S., Yin, Z., Tian, S., Li,

523 J.J.I.j.o.e.r., health, p., 2017b. Adsorption removal of 17β-estradiol from water by rice

524 straw-derived biochar with special attention to pyrolysis temperature and background

525 chemistry. 14, 1213.

526 Wang, Y., Li, Q., Zhang, P., O'Connor, D., Varma, R.S., Yu, M., Hou, D., 2019c.

527 One-pot Green Synthesis of Bimetallic Hollow Palladium-platinum Nanotubes for

528 Enhanced Catalytic Reduction of p–Nitrophenol. Journal of Colloid and Interface

529 Science.

530 Wei, S., Zhu, M., Fan, X., Song, J., Peng, P., Li, K., Jia, W., Song, H., 2019. Influence of

531 pyrolysis temperature and feedstock on carbon fractions of biochar produced from

532 pyrolysis of rice straw, pine wood, pig manure and sewage sludge. Chemosphere 218,

533 624-631.

534 Yuan, H., Lu, T., Wang, Y., Huang, H., Chen, Y., 2014. Influence of pyrolysis

535 temperature and holding time on properties of biochar derived from medicinal herb

536 (radix isatidis) residue and its effect on soil CO2 emission. Journal of Analytical and

537 Applied Pyrolysis 110, 277-284.

538 Zhang, F., Wang, X., Yin, D.X., Peng, B., Tan, C.Y., Liu, Y.G., Tan, X.F., Wu, S.X., 2015.

539 Efficiency and mechanisms of Cd removal from aqueous solution by biochar derived
540 from water hyacinth (Eichornia crassipes). Journal of Environmental Management 153,
541 68-73.
542 Zhang, H., Chen, C., Gray, E.M., Boyd, S.E., 2017. Effect of feedstock and pyrolysis
543 temperature on properties of biochar governing end use efficacy. Biomass and
544 Bioenergy 105, 136-146.
545 Zhang, P., Hou, D., O'Connor, D., Li, X., Pehkonen, S.O., Varma, R.S., Wang, X., 2018.
546 Green and Size-Specific Synthesis of Stable Fe-Cu Oxides as Earth-Abundant
547 Adsorbents for Malachite Green Removal. ACS Sustainable Chemistry & Engineering,
548 9229-9236.
549 Zhang, Y., Hou, D., O'Connor, D., Shen, Z., Shi, P., Ok, Y.S., Tsang, D.C.W., Wen, Y.,
550 Luo, M., 2019. Lead contamination in Chinese surface soils: Source identification,
551 spatial-temporal distribution and associated health risks AU - Zhang, Yunhui. Critical
552 Reviews in Environmental Science and Technology, 1-38.
553 Zhao, B., O'Connor, D., Zhang, J., Peng, T., Shen, Z., Tsang, D.C.W., Hou, D., 2018.
554 Effect of pyrolysis temperature, heating rate, and residence time on rapeseed stem
555 derived biochar. Journal of Cleaner Production 174, 977-987.
556 Zhao, S.X., Ta, N., Wang, X.D., 2017. Effect of Temperature on the Structural and
557 Physicochemical Properties of Biochar with Apple Tree Branches as Feedstock Material.
558 Energies 10.
559 Zhao, X., Zhang, J.J.F.L.C., 2013. Review of regulatory frameworks for contaminated

land in China. 8, 69.

List of tables

Table 1 Biochar properties

	CRSB300	CRSB500	CRSB700
Yield	44.0%	31.9%	29.8%
pH	7.50±0.03	10.4±0.01	10.5±0.01
BET surface area (m^2/g)	1.76	3.80	188
Average pore width	65.38	40.33	6.98

(nm)[b]			
C (%)	49.9±0.2	52.2±0.1	53.3±0.1
H (%)	3.38±0.01	2.25±0.01	1.39±0.03
N (%)	1.52±0.01	1.31±0.01	1.13±0.01
O (%)	19.6±0.1	11.6±0.03	7.95±0.08
H/C	0.0677	0.0431	0.0261
O/C	0.393	0.222	0.149

588 a- mean ± standard deviation, n=2

589 b - BJH Adsorption average pore width (4V/A)

590

591

592 Table 2 Kinetics parameters for cadmium removal by the biochars

Biochar	Pseudo first order			Pseudo second order			Intraparticle diffusion		
	q_e (mg/g)	k_1 (h^{-1})	R^2	q_e (mg/g)	k_2 (g/mg h)	R^2	k_1 (mg/g $h^{-0.5}$)	k_2 (mg/g $h^{-0.5}$)	k_3 (mg/g $h^{-0.5}$)
CRSB300	21.8	0.79	0.80	23.8	0.05	0.90	49.2	4.54	-1.56
CRSB5	36.2	8.10	0.43	38.2	0.31	0.74	17.0	4.22	-0.878

00									
CRSB700	48.7	10.87	0.58	50.8	0.35	0.84	25.7	3.84	1.68

593

594

595

596

597

598

599

600

601

602

603 Table 3 Parameters obtained from isotherm fitting using Langmuir and

604 Freundlich models

Biochar	Langmuir			Freundlich		
	Q_{max} (mg/g)	b (L/mg)	R^2	K_f (mg/g)	1/n	R^2

CRSB300	21.4	1.21	0.98	9.27	0.16	0.83
CRSB500	44.2	0.77	0.82	14.40	0.23	0.83
CRSB700	65.5	3.83	0.48	28.76	0.15	0.29

605

606

607

608

609

610

611

612

613

614 List of figures

619 biochars (CRS-cadmium contaminated rice straw, CRSB-cadmium
620 contaminated rice straw biochar produced at different temperatures)

621 Figure 5 Fractions (a) and concentrations (b) of cadmium immobilized on the
622 biochars

623 Figure 6 Kinetics results of cadmium removal by the biochars

624 Figure 7 Equilibrium results of cadmium removal by the biochars

625

626

627

628

629

630

631

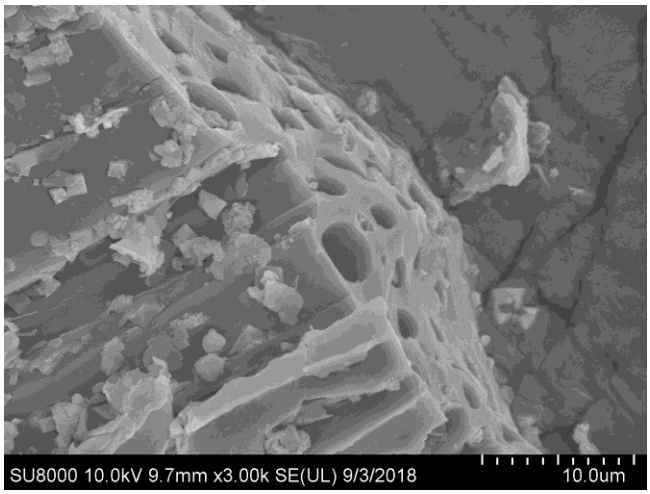

(a) CRSB300

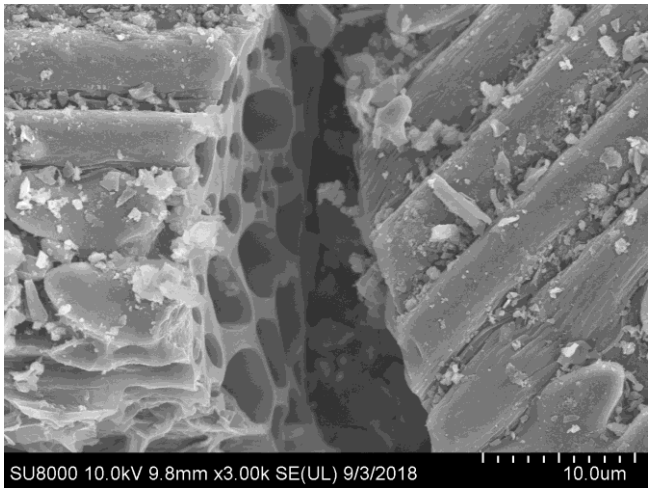

(b) CRSB500

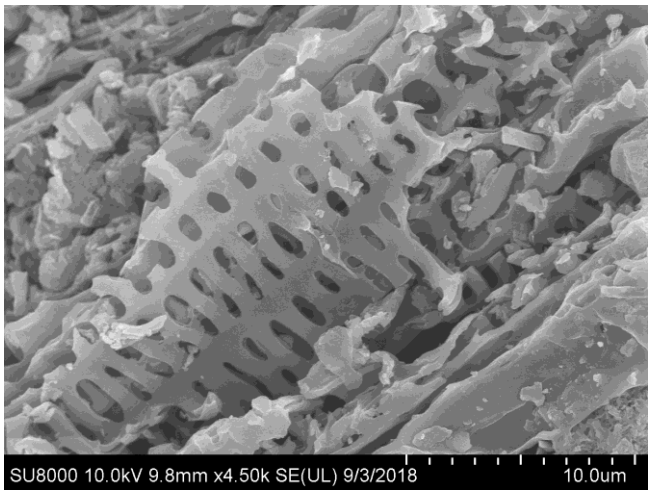

(c) CRSB700

632 Figure 1 surface morphology of the biochars

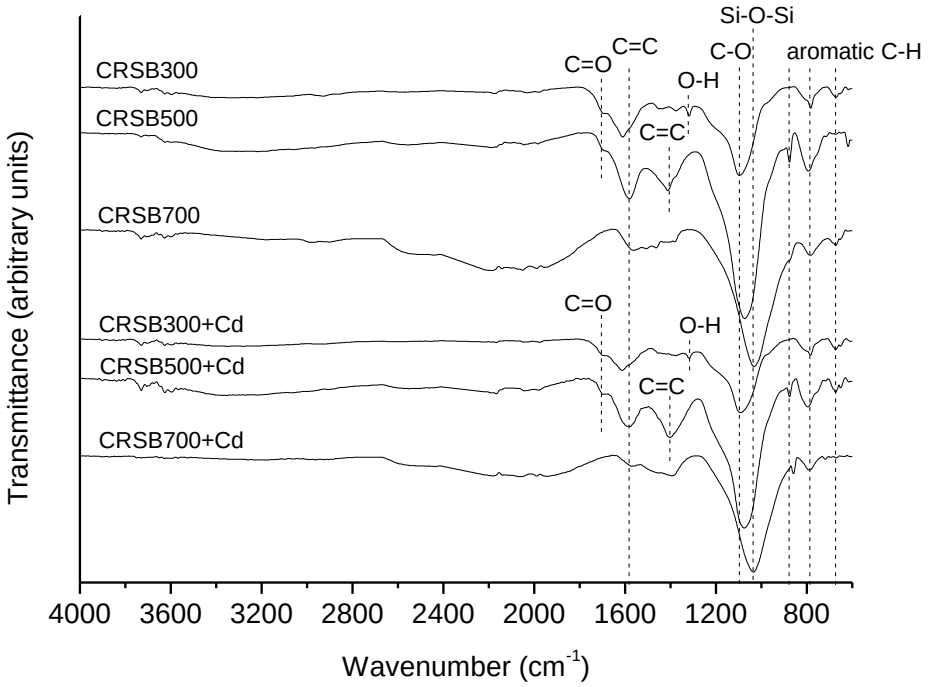

633

634 Figure 2 Biochar FTIR spectra before and post Cd immobilization

635

636

637

638

639

640

641

642

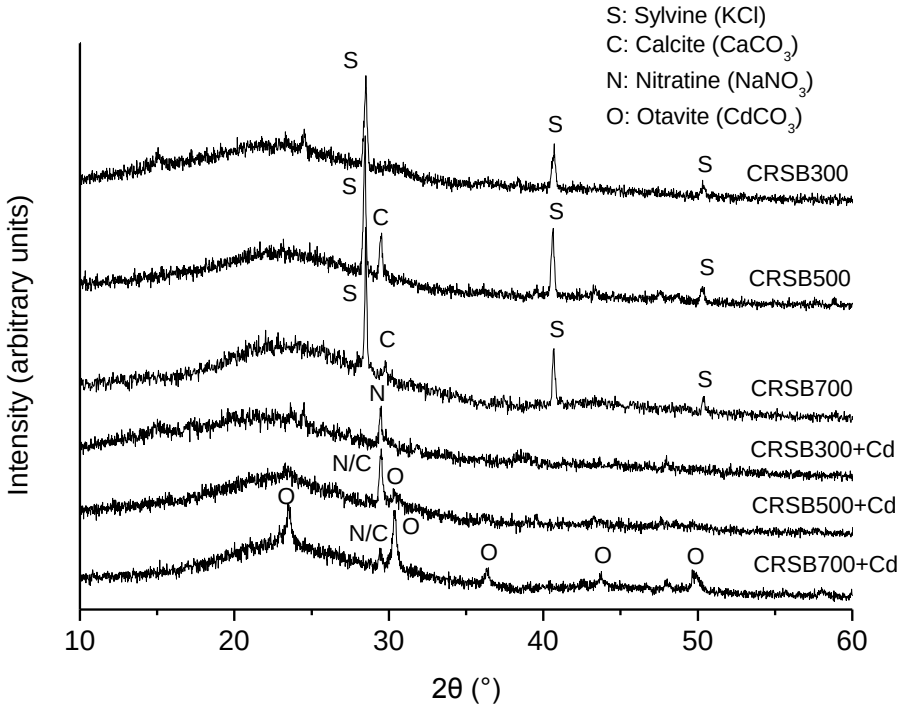

643

644 Figure 3 Biochar XRD patterns before and post Cd immobilization

645

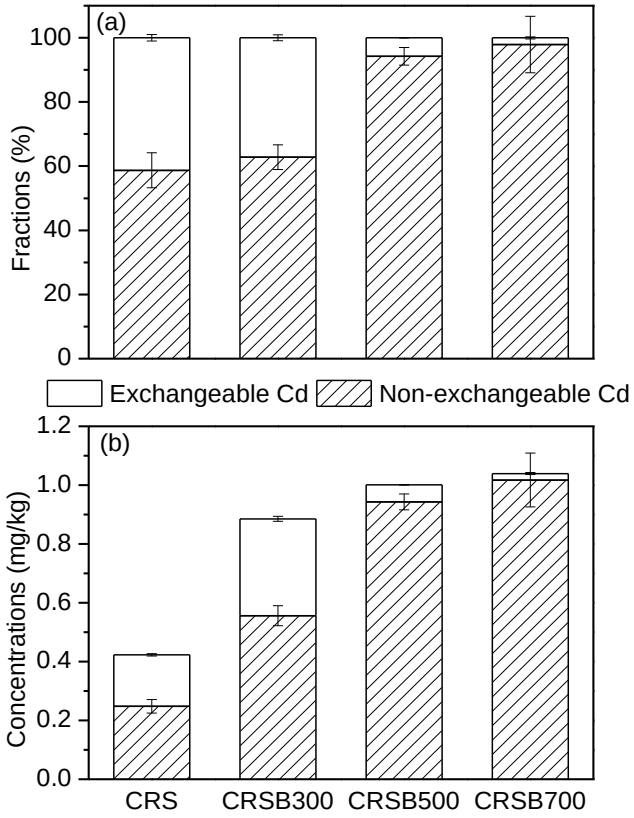

646

647 Figure 4 Fractions (a) and concentrations (b) of cadmium remained in the

648 biochars (CRS-cadmium contaminated rice straw, CRSB-cadmium

649 contaminated rice straw biochar produced at different temperatures)

650

651

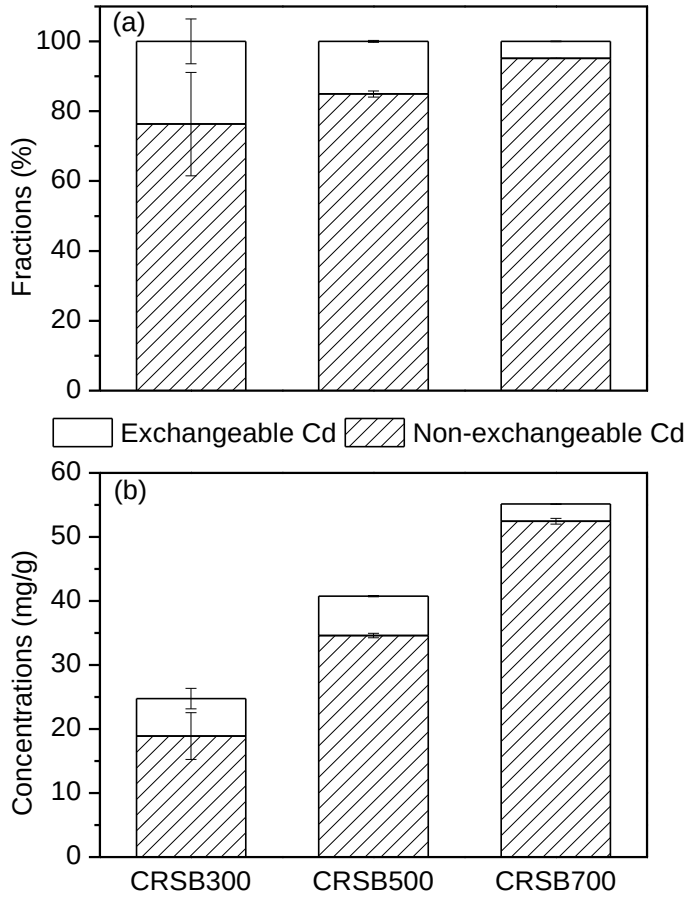

652

653 Figure 5 Fractions (a) and concentrations (b) of cadmium immobilized on the

654 biochars

655

656

657

658

659

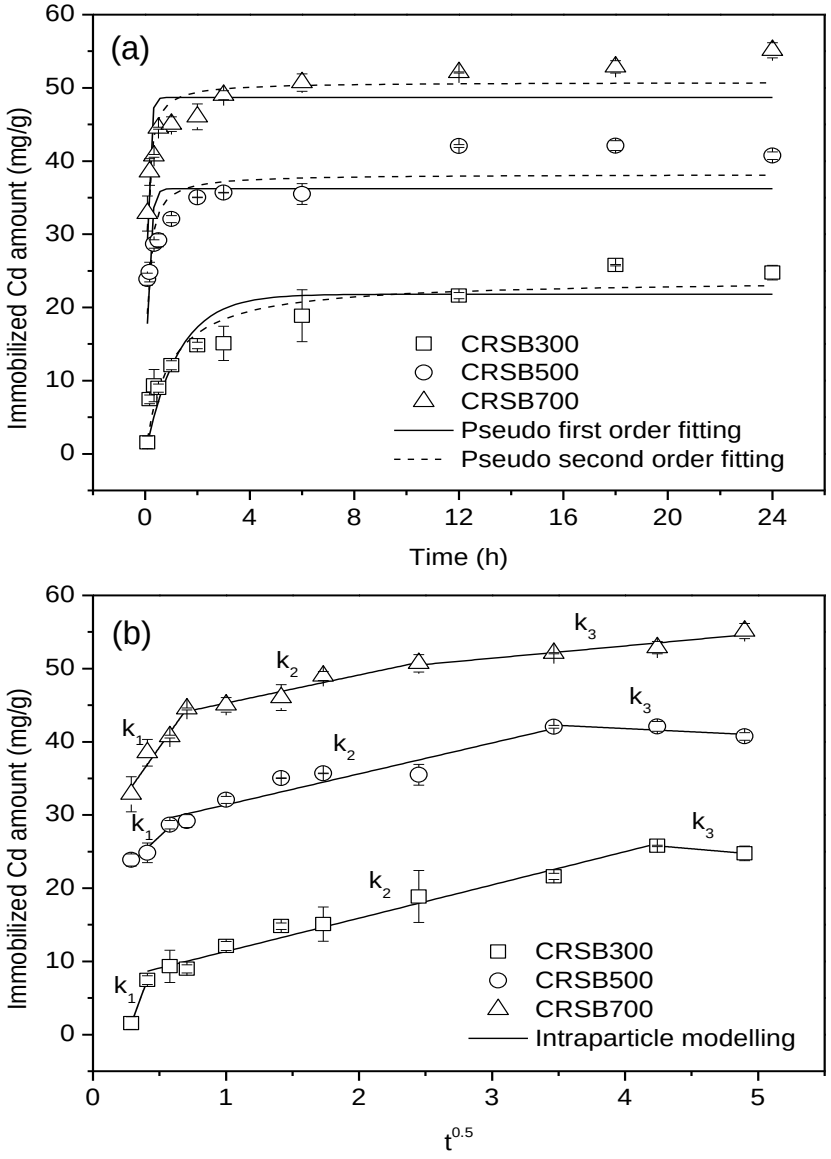

660

661 Figure 6 Kinetics results of cadmium removal by the biochars: (a) immobilized

662 Cd amount as a function of time, (b) intraparticle diffusion modelling

663

664

665

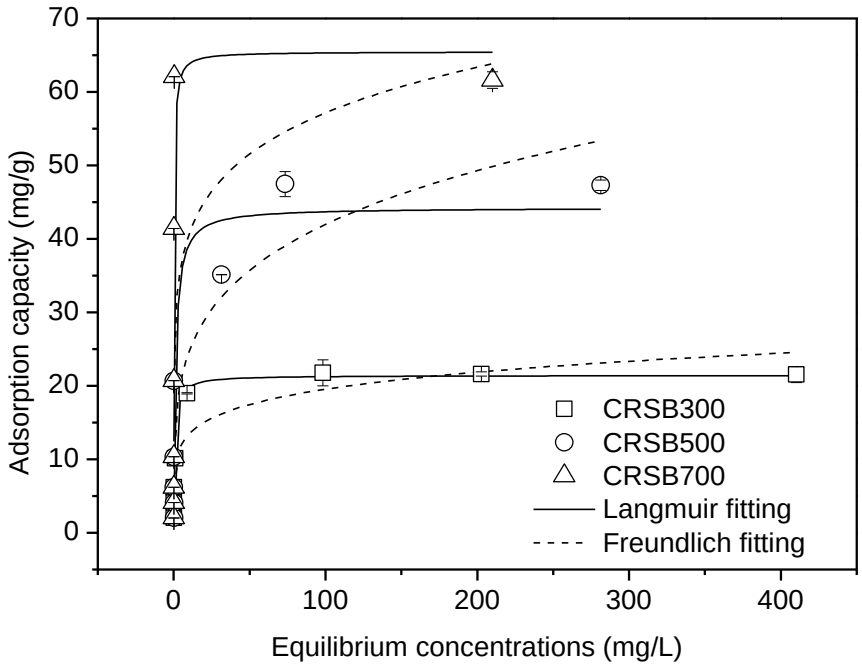

666

667 Figure 7 Equilibrium results of cadmium removal by the biochars

668